The 3.5 keV line: an unknown plasma line or a dark matter decay line?

March 2015

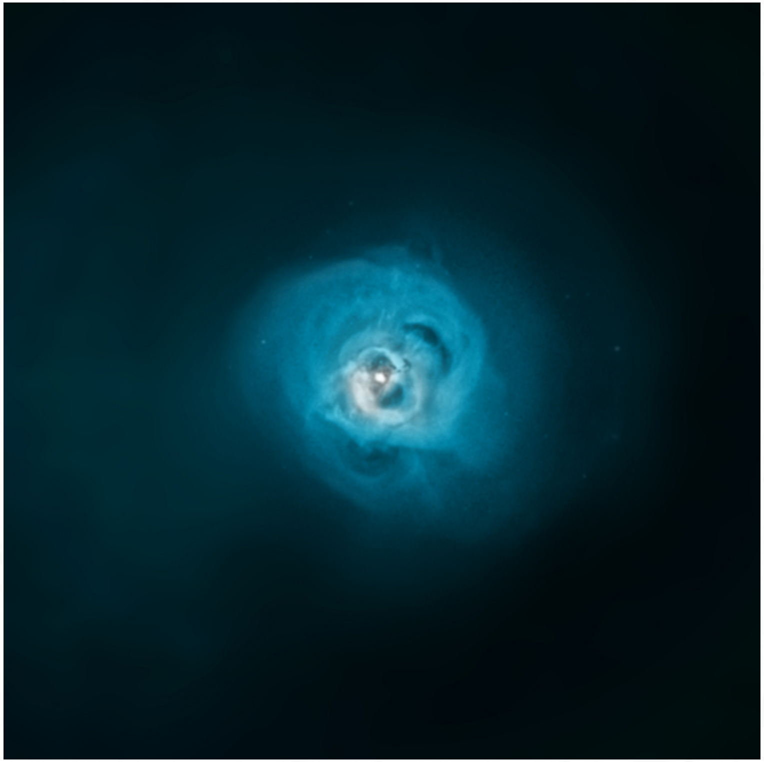

Bulbul et al 2014: Detection of an unidentified emission line in the stacked X-ray spectrum of galaxy clusters

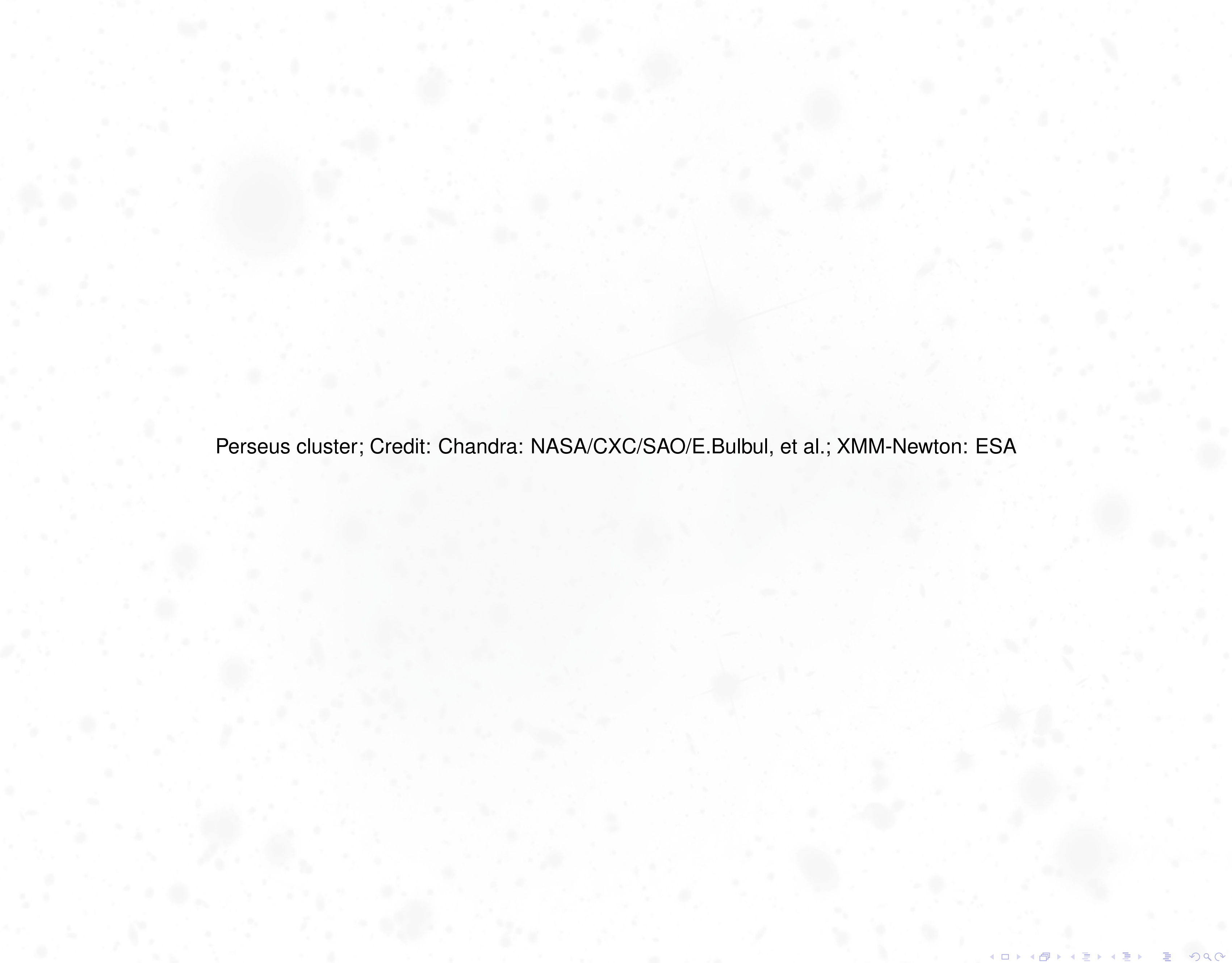

Perseus cluster; Credit: Chandra: NASA/CXC/SAO/E.Bulbul, et al.; XMM-Newton: ESA

Table of contents

Bulbul et al 2014

- A one year-old paper with 160 citations.
- Signal = Stacking of 73 rest frame and background-corrected X-ray spectra from galactic clusters detected by the EPIC camera of the XMM-Newton satellite.
- Detection of a significant unknown line (no explanation by existing plasma lines) at 3.5 keV.
- Possible explanation by the sterile neutrino decay.

Overview

Bulbul et al 2014

- A one year-old paper with 160 citations.
- Signal = Stacking of 73 rest frame and background-corrected X-ray spectra from galactic clusters detected by the EPIC camera of the XMM-Newton satellite.
- Detection of a significant unknown line (no explanation by existing plasma lines) at 3.5 keV.
- Possible explanation by the sterile neutrino decay.

XMM-Newton

- XMM: Two CCD cameras with two tech, MOS and PN.
- Energy range: 0.15-12 keV (MOS and PN)
- Energy resolution: $\sim$70 eV (MOS), $\sim$80 eV (PN)

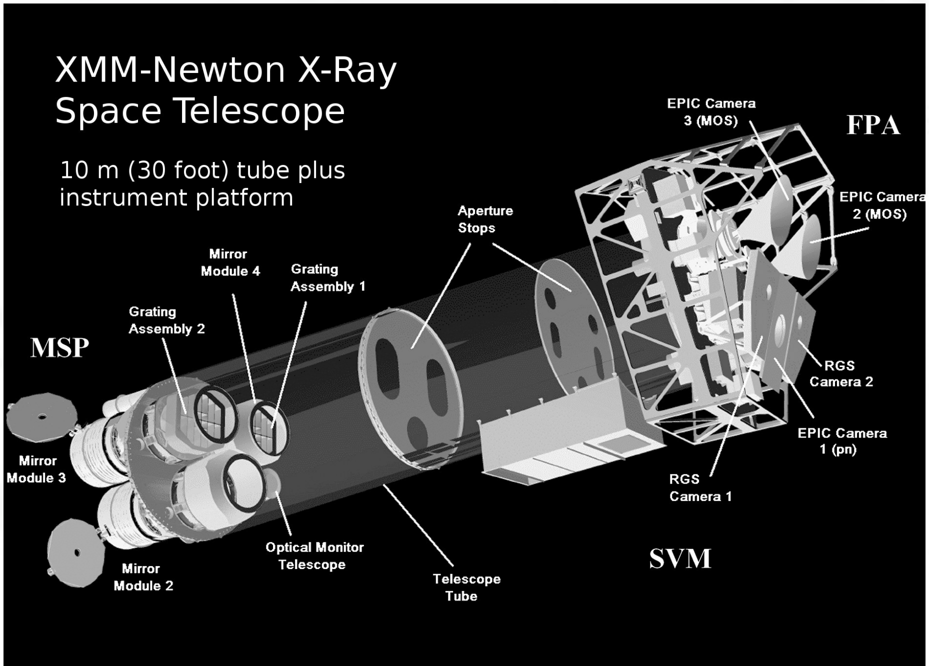

Table of contents

Data selection

73 clusters from XMM archive (Redshift range: 0.01-0.35). In order to have enough high-z clusters compare to low-z clusters (Redshift leverage):

- if z<0.1, minimal number of counts : 10^5 photons
- if z>0.1, minimal number of counts : 10^4 photons

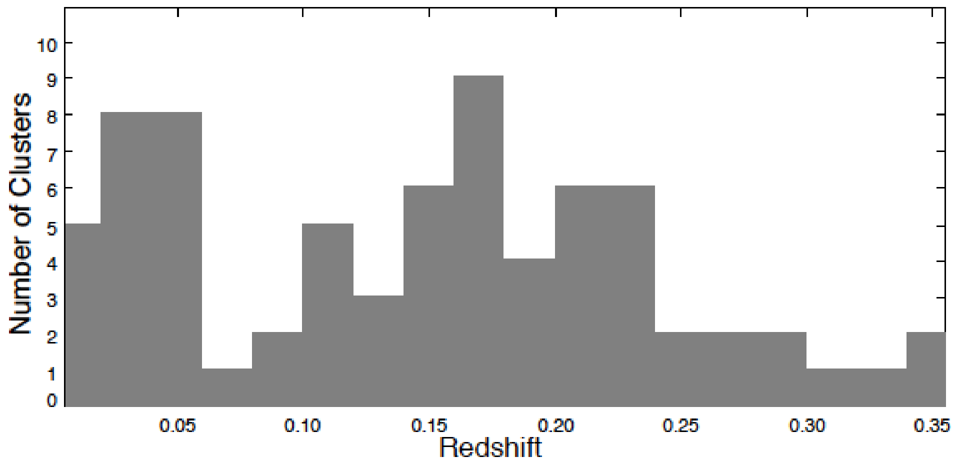

Data selection

73 clusters from XMM archive (Redshift range: 0.01-0.35). In order to have enough high-z clusters compare to low-z clusters (Redshift leverage):

- if z<0.1, minimal number of counts : 10^5 photons
- if z>0.1, minimal number of counts : 10^4 photons

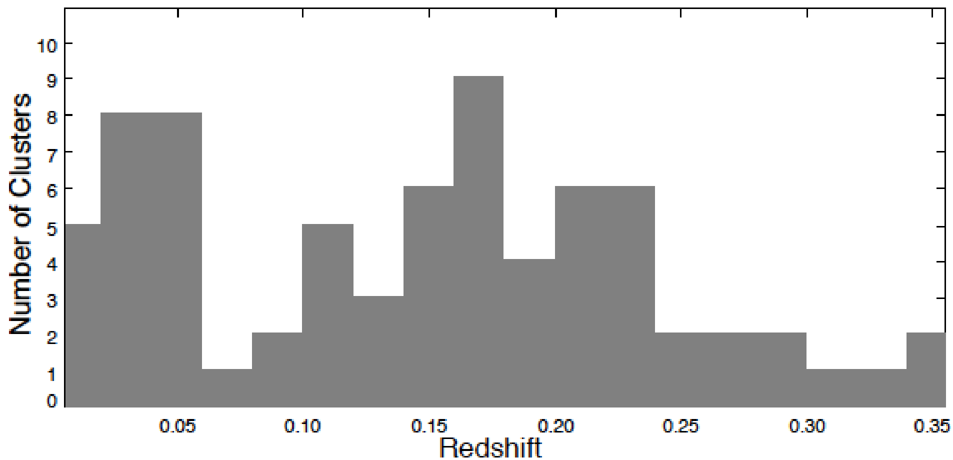

Signal extraction

- Selection of low background intervals of time $\rightarrow$ timelines of counts for each pixel and bands + clean exposure time
- Build sky map of counts in the 0.4-7.0 keV band
- Detection and exclusion of point sources (mainly AGN contamination)
- Spectra extracted from the counts within R_{500} (average density within the sphere > 500 times the critical density).

Building of the stacked spectra

Background modeling : continuum

- Soft X-ray background estimated from the outskirt of the cluster in the ROSAT All-sky survey maps.
- Local hot bubble and heliosphere: cool unabsorbed single-temperature thermal component model.
- Galactic hotter halo + intergalactic medium : absorbed thermal component model.
- Unresolved point source effect contamination modeled by a power law.

Building of the stacked spectra

Background modeling : continuum

- Soft X-ray background estimated from the outskirt of the cluster in the ROSAT All-sky survey maps.
- Local hot bubble and heliosphere: cool unabsorbed single-temperature thermal component model.
- Galactic hotter halo + intergalactic medium : absorbed thermal component model.
- Unresolved point source effect contamination modeled by a power law.

Background modeling : instrumental lines

- Quiescent particles background for MOS: Al-K (1.49 keV) and Si-K (1.74 keV) fluorescent lines $\rightarrow$ Gaussian fits
- Quiescent particles background for PN: Al-K (1.49 keV), Ni-K(7.48 keV), Cu-K(8.05, 8.91 keV) and Zn-K (8.64, 9.57 keV) fluorescent lines $\rightarrow$ Gaussian fits

Two upper curves: Perseus spectra; two lower curves: estimated Perseus background

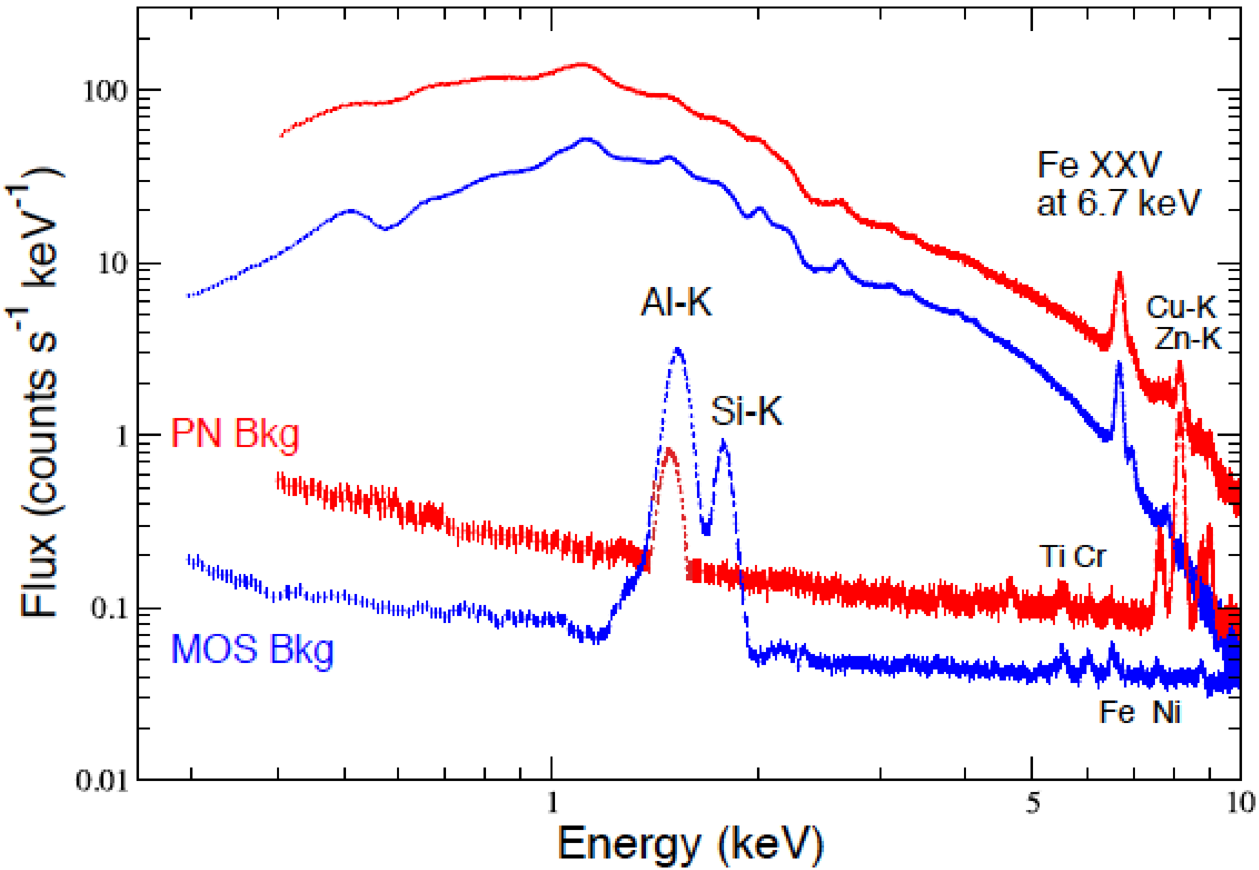

Redshift estimation

- Individual fit of the background-subtracted signal; continuum with an absorbed multi-temperature equilibrium plasma; bright lines with the AtomDB database (http://www.atomdb.org)
- Redshift determination with the bright Fe found lines.

Redshift estimation

- Individual fit of the background-subtracted signal; continuum with an absorbed multi-temperature equilibrium plasma; bright lines with the AtomDB database (http://www.atomdb.org)
- Redshift determination with the bright Fe found lines.

Smearing effect for the weak instrumental lines

- All the spectra are set in the rest frame (z=0)and are stacked.
- Enough high-z clusters: amplification of the plasma lines, no amplification of the instrumental lines (smearing effect)
- Possible smoothing of the quantum efficiency unknown variation.

Stacking the signal smears out the instrumental lines.

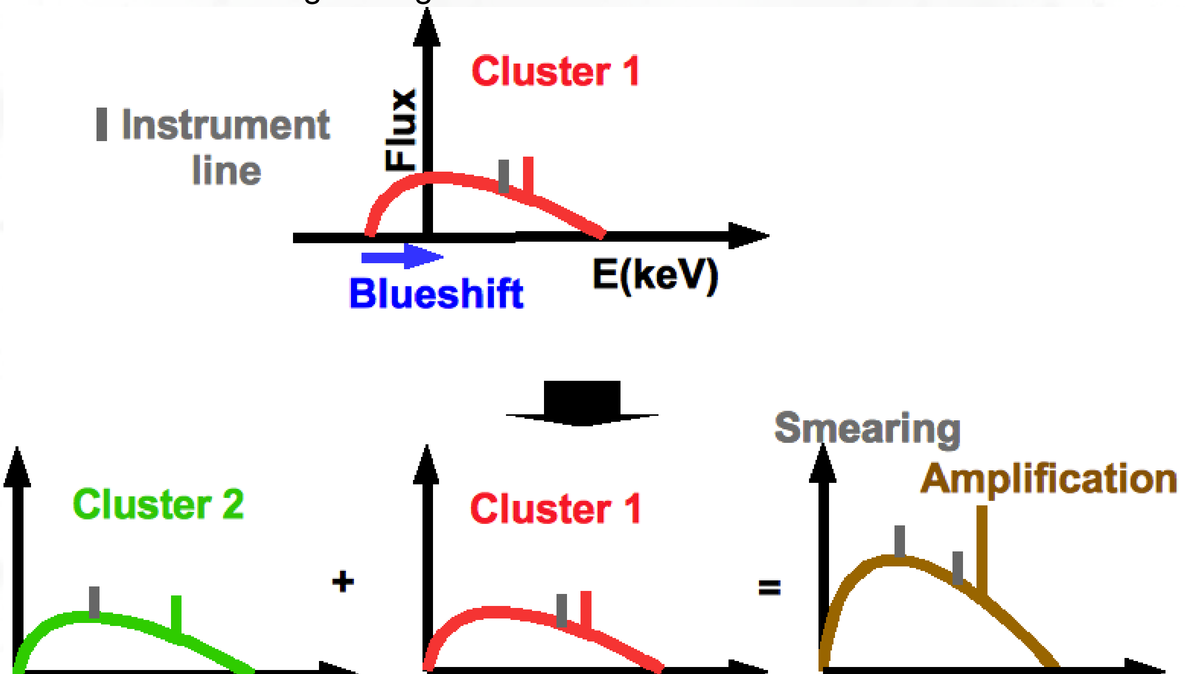

Weak instrumental lines are smeared out in the stacked signal compare to the Perseus signal.

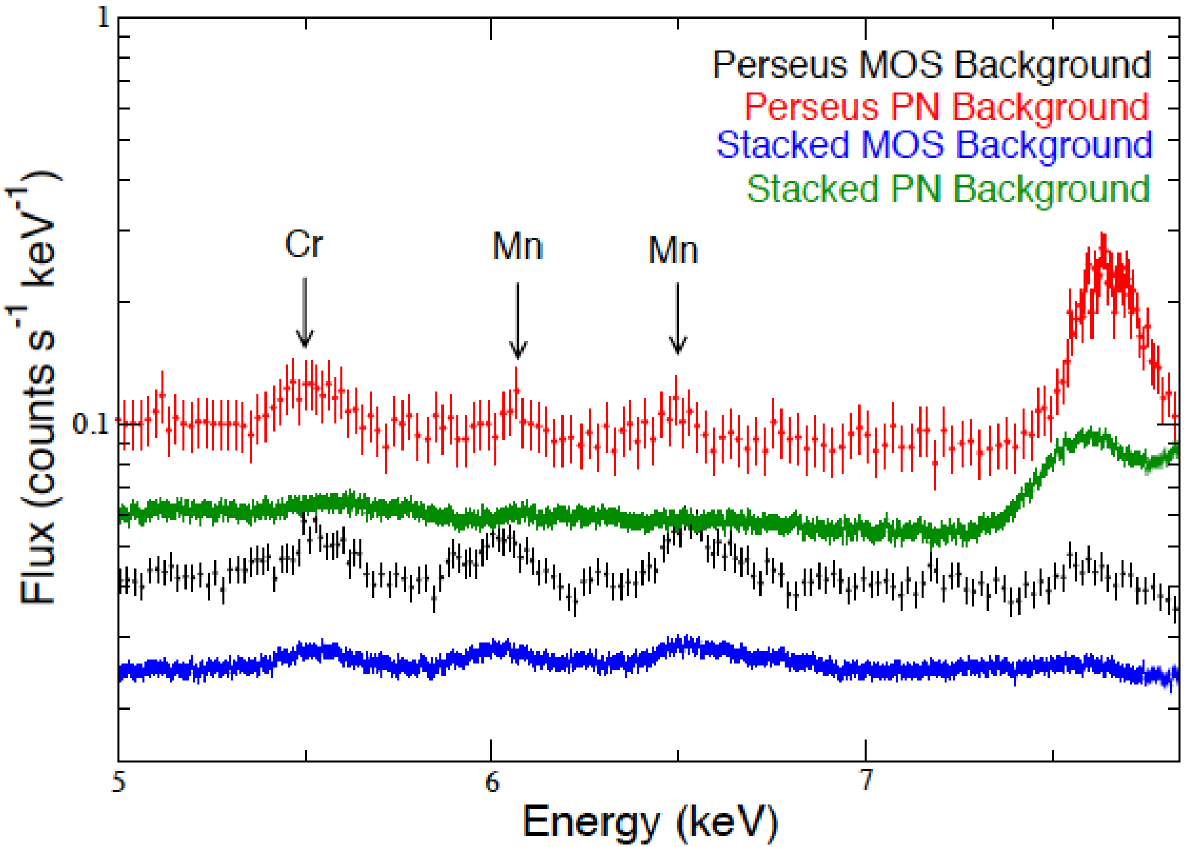

Table of contents

Signal fitting by AtomDB

Fitting procedure

- Fit of the continuum spectrum by a 4 Bremsstrahlung emission models.
- Fit of the strong plasma lines by Gaussian curves.
- Estimation of the range of the flux of the weak plasma lines around 3.5 keV and fit by Gaussian curves.

Fitting procedure

- Fit of the continuum spectrum by a 4 Bremsstrahlung emission models.
- Fit of the strong plasma lines by Gaussian curves.
- Estimation of the range of the flux of the weak plasma lines around 3.5 keV and fit by Gaussian curves.

Continuum

- Continuum: Bremsstrahlung (free-free electrons/ions) and radiative recombination (free-bound). For hot collisional plasma (kT>0.1 keV): Bremsstrahlung dominant.
- Fit with a collisional plasma model in thermal equilibrium "Apec" from AtomDB with a flux $F[photon.cm^{-2}.s^{-1}] = \varepsilon(T_e)N$. Emissivity $\varepsilon(T_e)[photon.cm^3.s^{-1}] \propto f(E)T_e^{1/2}$ (for Bremsstrahlung)
- Normalization $N[cm^{-5}] = \frac{\int n_e n_h dV}{4\pi D_L^2}$ for one cluster at redshift z with n_e, n_h and D_L respectively the electronic density, the hydrogen density and the luminosity distance.
- Fit with 4 different models with the temperatures and the normalization as free parameters. Temperatures for MOS: 5.9-6.1-7.3-10.9 (keV); Temperatures for PN: 2.3-6.9-7.3-18.7 (keV).
- Power-law to fit the soft photons contamination.

Free-free emission.

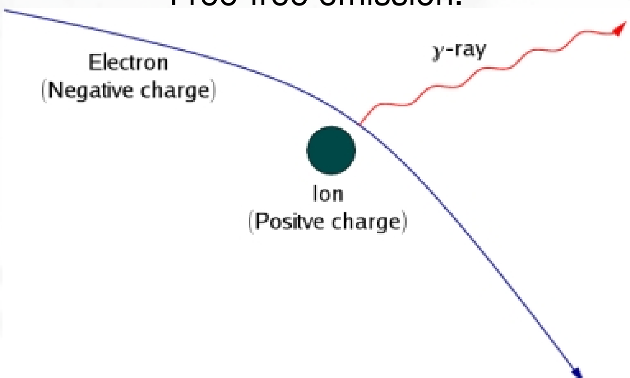

Plasma lines

- In highly ionized plasma, large amount of ions with 1,2 or 3 bound electrons $\rightarrow$ H-like, He-like lines or Li-like lines (and dielectric recombination lines).
- Model for plasma line $F[photon.cm^{-2}.s^{-1}] = \varepsilon(T_e)N$ (AtomDB formalism)
- Emissivity $\varepsilon(T_e) \propto n_k A_{i,j}$ with n_k the density of the ion in the state k and $A_{j,k}$ the atomic transition probability from the state j to the state k.

Signal fitting by AtomDB

Plasma lines

- In highly ionized plasma, large amount of ions with 1,2 or 3 bound electrons electrons $\rightarrow$ H-like, He-like lines or Li-like lines (and dielectric recombination lines).
- Model for plasma line $F[photon.cm^{-2}.s^{-1}] = \varepsilon(T_e)N$ (AtomDB formalism)
- Emissivity $\varepsilon(T_e) \propto n_k A_{i,j}$ with n_k the density of the ion in the state k and $A_{j,k}$ the atomic transition probability from the state j to the state k.

n_k element density estimation

- $n_k = \frac{n_k}{n_z}\frac{n_z}{n_Z}\frac{n_Z}{n_h}\frac{n_h}{n_e} n_e$
- $n_k/n_z = p_k$: % of the ions in the state k (depends on T_e, see below)
- n_z/n_Z : ionization balance (close to 1)
- n_Z/n_h : elemental abundance relative to hydrogen (Bulbul et al : solar photosphere)
- n_h/n_e : fraction of hydrogen to electron (0.8 for cosmic plasma).

Signal fitting by AtomDB

Plasma lines

- In highly ionized plasma, large amount of ions with 1,2 or 3 bound electrons $\rightarrow$ H-like, He-like lines or Li-like lines (and dielectric recombination lines).
- Model for plasma line $F[photon.cm^{-2}.s^{-1}] = \varepsilon(T_e)N$ (AtomDB formalism)
- Emissivity $\varepsilon(T_e) \propto n_k A_{i,j}$ with n_k the density of the ion in the state k and $A_{j,k}$ the atomic transition probability from the state j to the state k.

n_k element density estimation

- $n_k = \frac{n_k}{n_z}\frac{n_z}{n_Z}\frac{n_Z}{n_h}\frac{n_h}{n_e}n_e$
- $n_k/n_z = p_k$: % of the ions in the state k (depends on T_e, see below)
- n_z/n_Z : ionization balance (close to 1)
- n_Z/n_h : elemental abundance relative to hydrogen (Bulbul et al : solar photosphere)
- n_h/n_e : fraction of hydrogen to electron (0.8 for cosmic plasma).

An example of the determination of p_k

- Simple case: element with two states.
- Collisional plasma in thermal equilibrium $n_e p_1 \gamma_{1,2} = n_e p_2 \gamma_{2,1} + p_2 A_{2,1}$ with $\gamma_{1,2}$ and $\gamma_{2,1}$ the collision excitation rate and the de-excitation rate respectively.
- $p1 + p2 = 1$
- $p1 = \frac{n_e\gamma_{2,1}+A_{2,1}}{n_e(\gamma_{1,2}+\gamma_{2,1})+A_{2,1}}$ and $p2 = \frac{n_e\gamma_{1,2}+A_{2,1}}{n_e(\gamma_{1,2}+\gamma_{2,1})+A_{2,1}}$
- Matrix inversion approach for three or more states.
- The AtomDB database provides the values of the $\gamma(T_e)$ and A rates for different elements (e.g. Ar XVII, K XVIII)

Signal fitting by AtomDB

Strong plasma lines

- Keep on significant lines: emissivity at the lower temperature up to $\varepsilon_{min} = 5 \times 10^{-19} photons.cm^3.s^{-1}$.
- AtomDB: 28 lines
- Fit with a Gaussian curve for each line , energy allowed to vary up to 5 eV (Gain uncertainties)
- First fit of the stacked signal using the continuum fit and the 28 Gaussian curves.

Signal fitting by AtomDB

Strong plasma lines

- Keep on significant lines: emissivity at the lower temperature up to $\varepsilon_{min} = 5 \times 10^{-19} photons.cm^3.s^{-1}$.
- AtomDB: 28 lines
- Fit with a Gaussian curve for each line , energy allowed to vary up to 5 eV (Gain uncertainties)
- First fit of the stacked signal using the continuum fit and the 28 Gaussian curves.

Weak plasma lines around 3.5 keV

- Five weak known lines around 3.5 keV : K XVIII (He-like, 3.47 keV), K XVIII (He-like, 3.51 keV), Ar XVII (Dielectric recombination DR, 3.62 keV), Ar XVII (He-like, 3.68 keV) and K XIX (H-like, 3.71 keV).
- Estimated fluxes of the He/H-like lines from the fluxes of the strong lines S XVI (H-like, 2.63 keV), Ca XIX (He-like, 3.90 keV) and Ca XX (H-like, 4.11 keV) and solar abundances of S, Ca, Ar and K.
- $F_w = F_s \sum Norm_i \frac{\varepsilon_w(T_{e,i})}{\varepsilon_s(T_{e,i})}$ with s a strong line and w a weak line.
- Take the maximum of the flux F_w. The flux must vary between 0.1- 3 times this maximum (abundance uncertainties).
- Ar XVII DR line: flux between 0.001 and 0.01 the flux of the He-like Ar XVII line at 3.12 keV.

Weak line flux estimated from the strong lines of S XVI, Ca XIX and Ca XX assuming solar abundances.

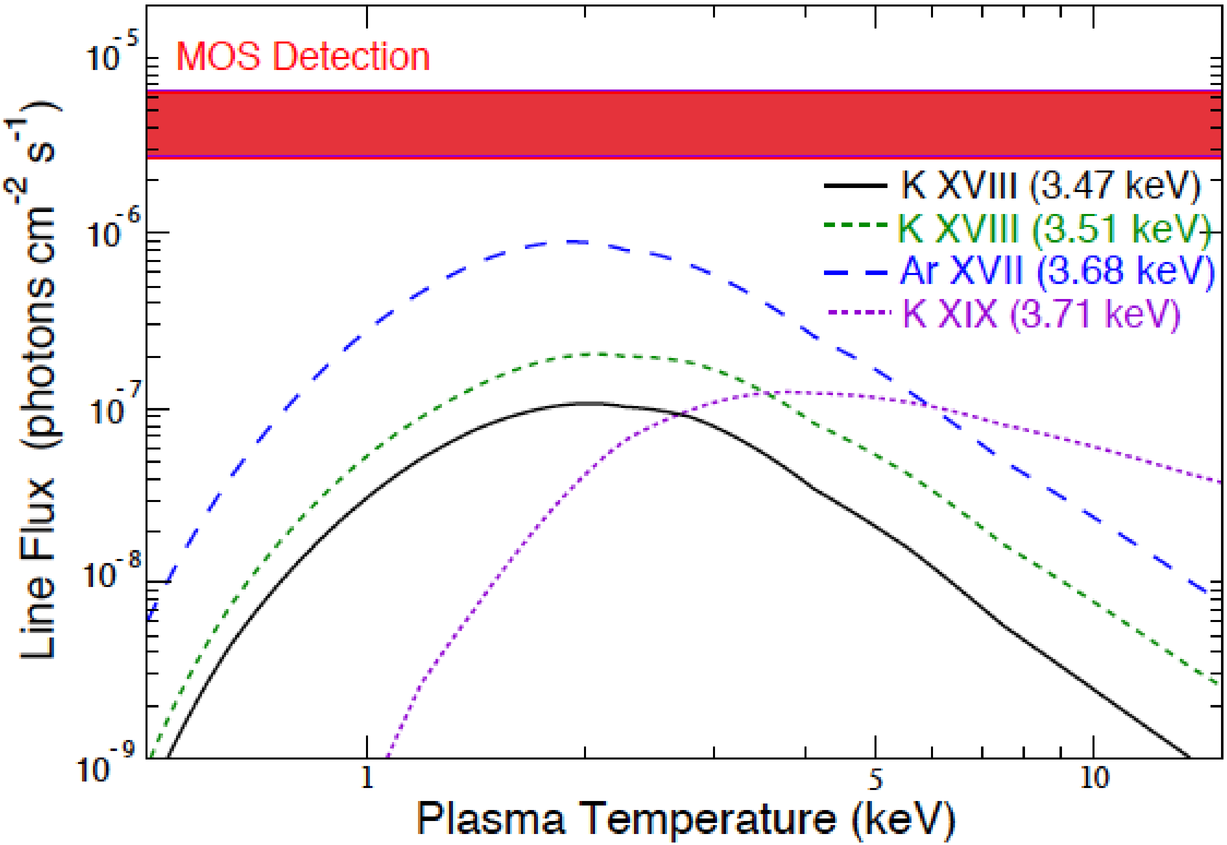

The Ar XVIII DR line emissivity compared to the Ar XVII line at 3.12 keV emissivity.

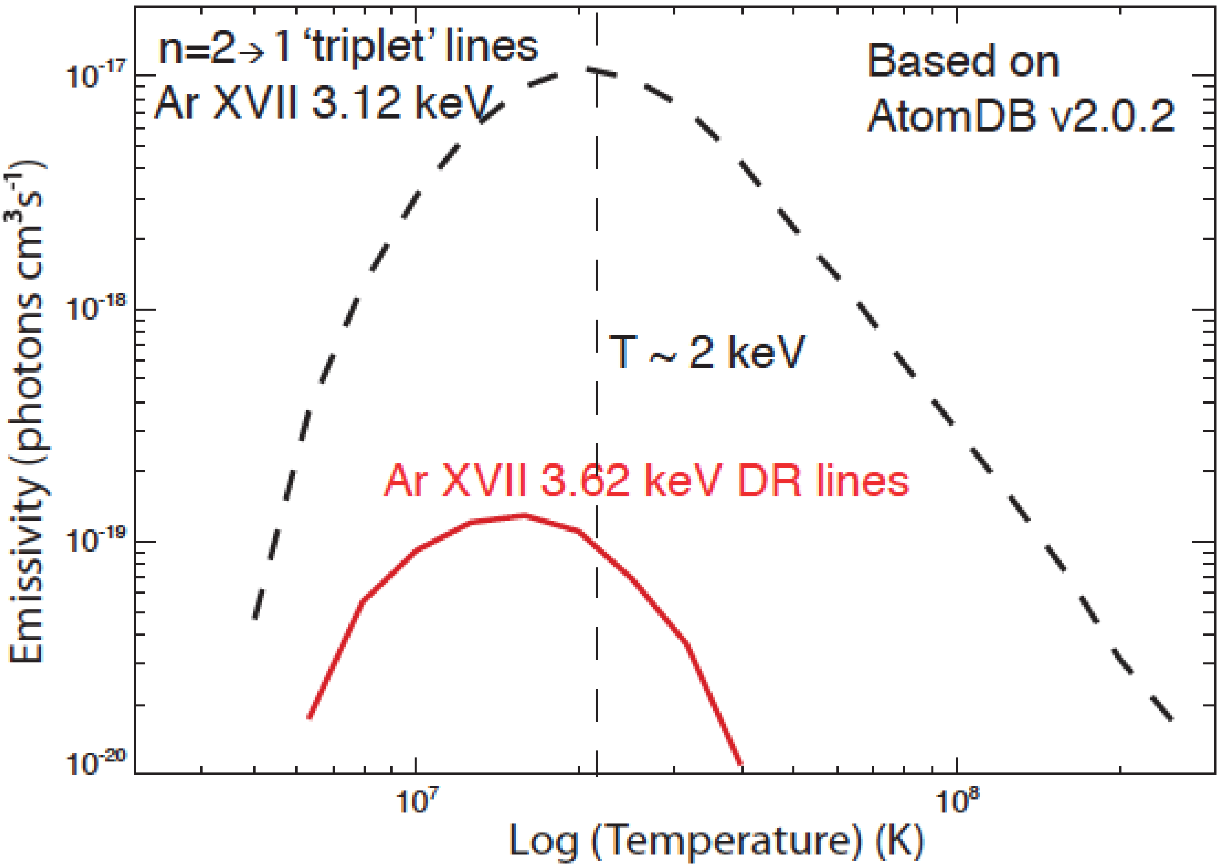

An unknown line at 3.5 keV

- Second fit (in the 3-6 keV energy band): Continuum+Strong lines +Weak lines (with respect to the last upper and lower limits); MOS channel: χ^2=564.8 (566 dof); PN channel: χ^2=510.5 (564 dof)
- Significant residual at 3.57$\pm$0.02 keV for the MOS channel and 3.51$\pm$0.03 for the PN channel (4-5 σ)
- The fit with a Gaussian curve with two parameters improves the $\Delta\chi^2$ of 22.8 for MOS and 13.9 for PN.
- Monte-carlo simulations of the PN signal: Improvement of the $\Delta\chi^2$ >11.2 in 0.4% of the cases in the lack of additional unknown line.

An unknown line at 3.5 keV

- Second fit (in the 3-6 keV energy band): Continuum+Strong lines +Weak lines (with respect to the last upper and lower limits); MOS channel: χ^2=564.8 (566 dof); PN channel: χ^2=510.5 (564 dof)
- Significant residual at 3.57$\pm$0.02 keV for the MOS channel and 3.51$\pm$0.03 for the PN channel (4-5 σ)
- The fit with a Gaussian curve with two parameters improves the $\Delta\chi^2$ of 22.8 for MOS and 13.9 for PN.
- Monte-carlo simulations of the PN signal: Improvement of the $\Delta\chi^2$ >11.2 in 0.4% of the cases in the lack of additional unknown line.

Rebinned spectra of the stacked clusters.

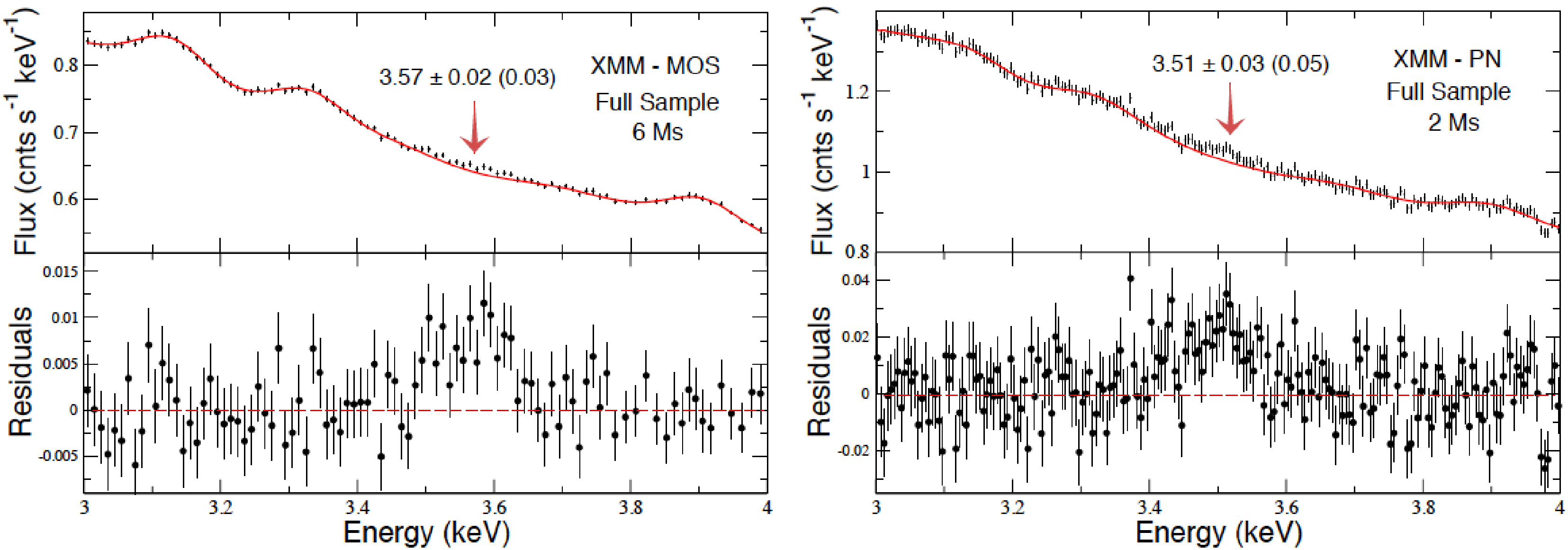

An unknown line at 3.5 keV

- Second fit (in the 3-6 keV energy band): Continuum+Strong lines +Weak lines (with respect to the last upper and lower limits); MOS channel: χ^2=564.8 (566 dof); PN channel: χ^2=510.5 (564 dof)
- Significant residual at 3.57$\pm$0.02 keV for the MOS channel and 3.51$\pm$0.03 for the PN channel (4-5 σ)
- The fit with a Gaussian curve with two parameters improves the $\Delta\chi^2$ of 22.8 for MOS and 13.9 for PN.
- Monte-carlo simulations of the PN signal: Improvement of the $\Delta\chi^2$ >11.2 in 0.4% of the cases in the lack of additional unknown line.

Rebinned spectra of the stacked clusters without the brightest of them.

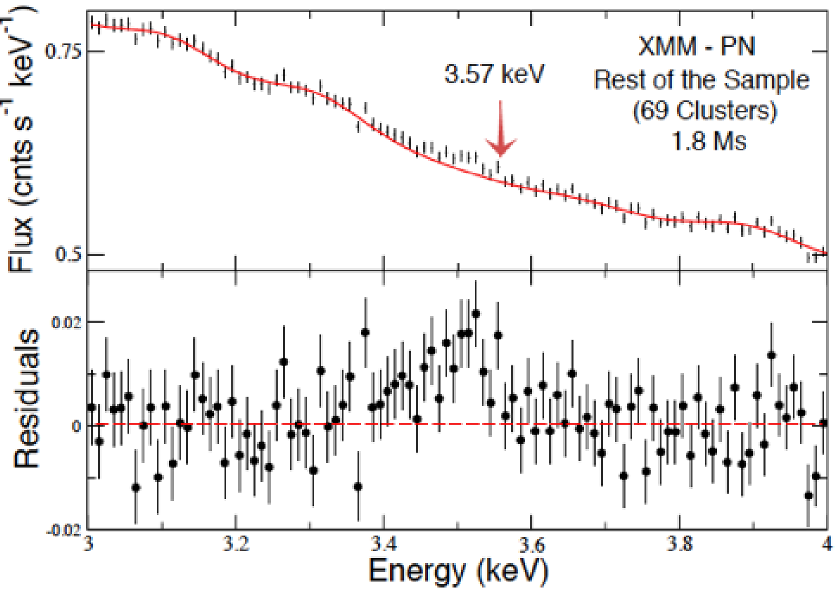

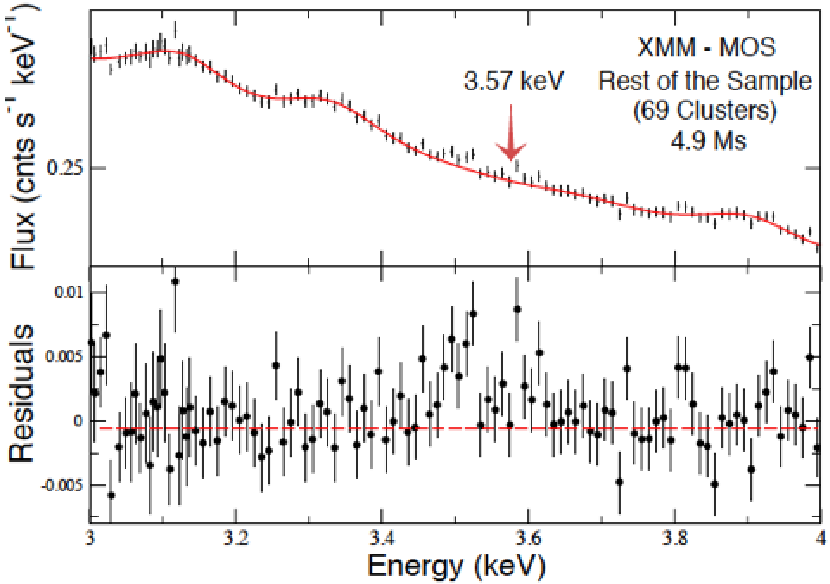

Table of contents

Few words for SUSY candidates

- Choi et al 2014: Decay of an axino with a mass $m_a = 7keV$ into a photon and a neutrino (warm dark matter candidate).
- Kang et al 2015: Other mechanisms: Dark gaugino which decays into two photons (Warm dark matter candidate). Cold dark matter particle which decays into a lighter one plus a photon.

Few words for SUSY candidates

- Choi et al 2014: Decay of an axino with a mass $m_a = 7keV$ into a photon and a neutrino (warm dark matter candidate).
- Kang et al 2015: Other mechanisms: Dark gaugino which decays into two photons (Warm dark matter candidate). Cold dark matter particle which decays into a lighter one plus a photon.

Sterile neutrino decay hypothesis

- A sterile neutrino with a mass m_s decays into a photons at an energy of $\frac{m_s c^2}{2}$ and an active neutrino. Here $m_s = 7.1keV$.
- Dark matter flux for one cluster : $F_{DM} = \frac{\Gamma_\gamma}{m_s} \frac{M_{DM}(<R)(1+z)}{4\pi D_L^2} = \frac{\Gamma_\gamma}{m_s} \mu_{DM}$
- with Γ_γ the sterile neutrino decay rate given by Pat & Wolfenstein 1982 :

$$\Gamma_\gamma = 1.38 \times 10^{-29} s^{-1} \frac{sin^2(2\theta)}{10^{-7}} \left(\frac{m_s}{1keV}\right)^5$$

Few words for SUSY candidates

- Choi et al 2014: Decay of an axino with a mass $m_a = 7keV$ into a photon and a neutrino (warm dark matter candidate).
- Kang et al 2015: Other mechanisms: Dark gaugino which decays into two photons (Warm dark matter candidate). Cold dark matter particle which decays into a lighter one plus a photon.

Sterile neutrino decay hypothesis

- A sterile neutrino with a mass m_s decays into a photons at an energy of $\frac{m_s c^2}{2}$ and an active neutrino. Here $m_s = 7.1keV$.
- Dark matter flux for one cluster : $F_{DM} = \frac{\Gamma_\gamma}{m_s} \frac{M_{DM}(<R)(1+z)}{4\pi D_L^2} = \frac{\Gamma_\gamma}{m_s} \mu_{DM}$
- with Γ_γ the sterile neutrino decay rate given by Pat & Wolfenstein 1982 :

$$\Gamma_\gamma = 1.38 \times 10^{-29} s^{-1} \frac{sin^2(2\theta)}{10^{-7}} \left(\frac{m_s}{1keV}\right)^5$$

Dark matter halo mass estimation

Scaling relations.

- $M_{DM} = M_{tot} - M_{gas} - M_*$
- Vikhlinin et al 2009 (Chandra): T_X(from spectroscopy) $\rightarrow M_{tot} = M_0 \left(\frac{T_X}{5keV}\right)^a E(z)^{-1}$
- Vikhlinin et al 2009 (Chandra): $M_{tot} \rightarrow M_{gas} = M_{tot}(f_{g,0} + \alpha log(\frac{M_{tot}}{10^{15} h^{-1} M_\odot}))$
- Gonzales et al 2013 : $M_{tot} \rightarrow M_* = a \left(\frac{M_{tot}}{10^{14} M_\odot}\right)^b$

Measurement of $sin^2(2\theta)$

- Number of photons from the dark matter haloes $S = \sum F_{DM,i} \times e_i \times A_i = \frac{\Gamma_\gamma}{m_s} \sum \mu_{DM,i} \times e_i \times A_i$
- e_i: exposure times; A_i ancillary area response [cm^2] for a photon of energy $\frac{E}{1+z_i}$
- S $\rightarrow \Gamma_\gamma \rightarrow sin^2(2\theta)$
- $sin^2(2\theta)$: some tensions between the full sample-rest of the sample /Perseus /Coma+Centaurus+Ophiuchus/Virgo

Consistence with previous studies.

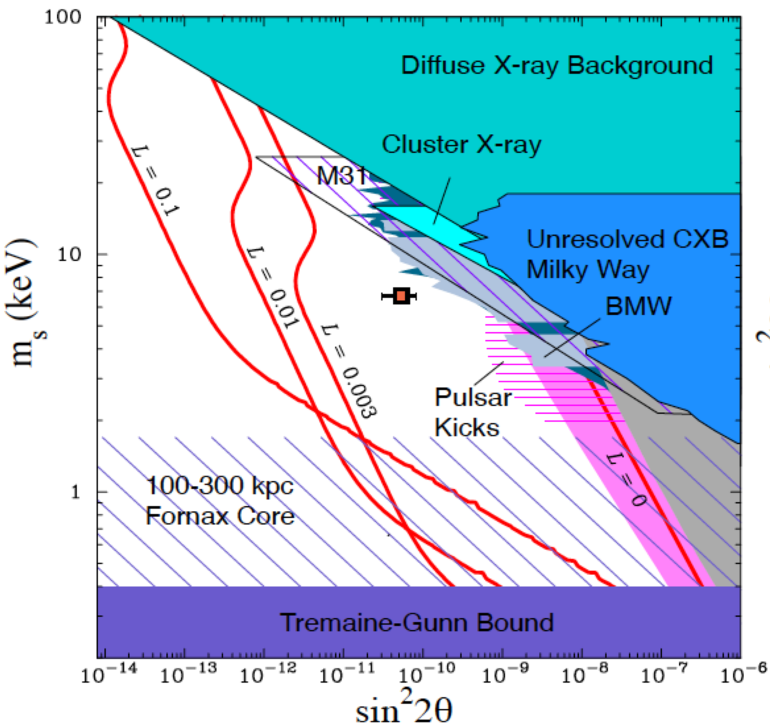

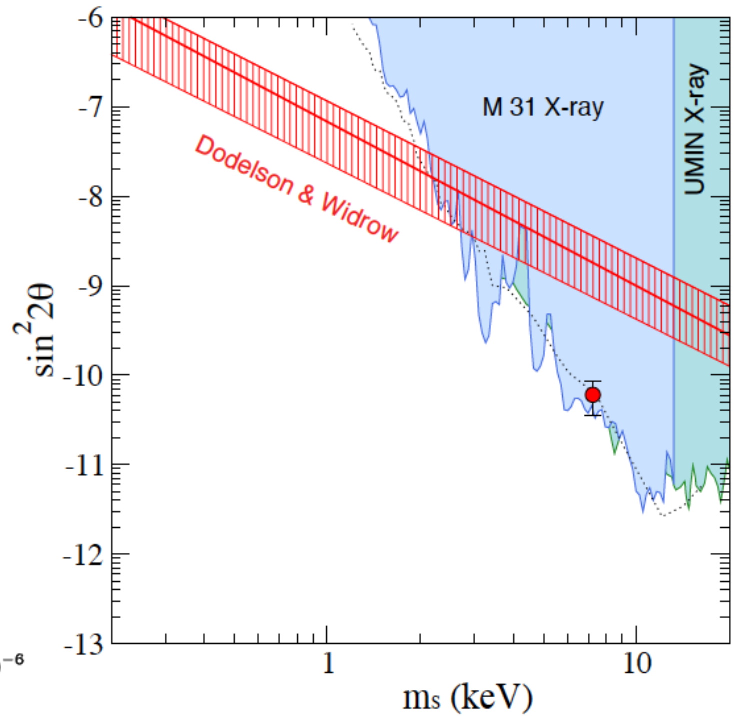

Measure of $sin^2(2\theta)$

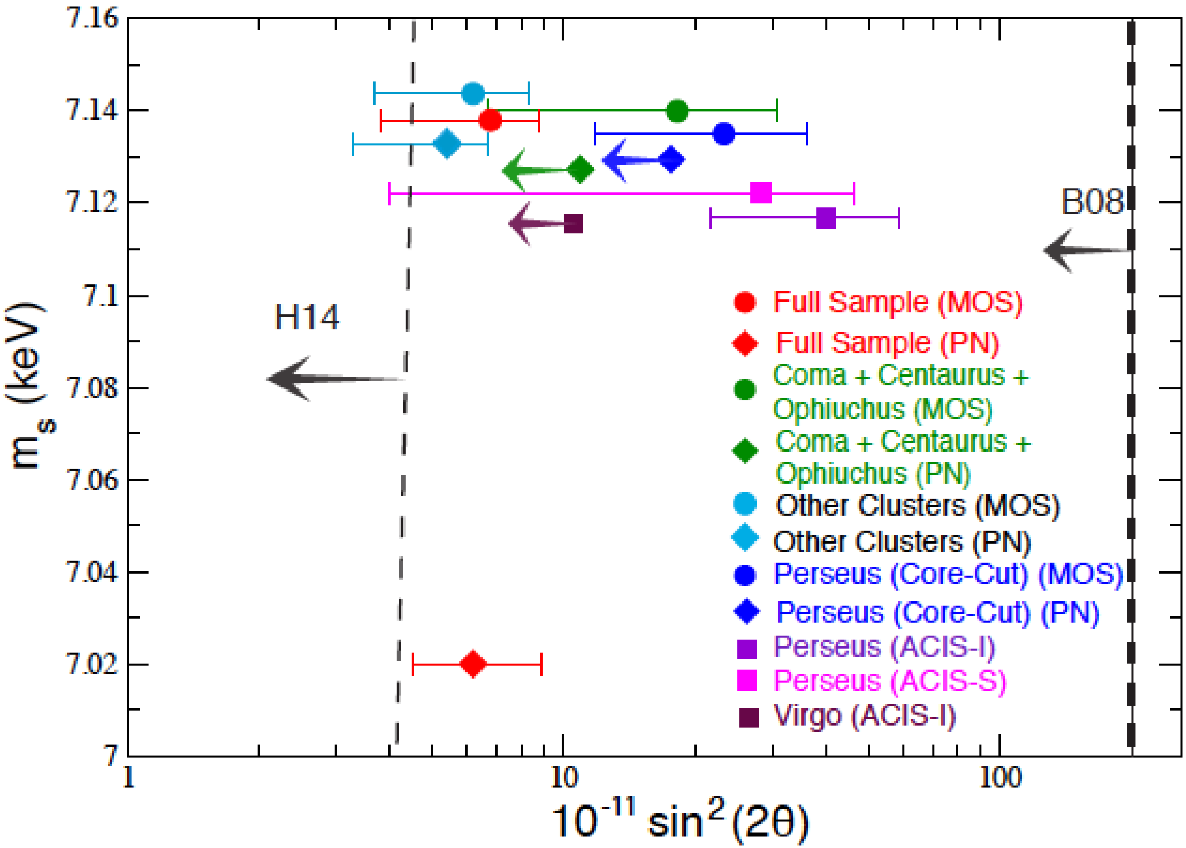

Table of contents

Possible candidates

- He-Like Cl line at 3.52 keV. But no presence of the stronger Cl lines at 3.27 keV and 3.44 keV.
- Underestimation of the K XVIII line (must be 10-20 times the estimated value to match with the unknown line).
- Non-equilibrium plasma: possible boost of the Ar XVII DR line at 3.62 keV (but not enough)
- S XVI recombination edge at 3.494 keV. Significant for colder electron $T_e \sim 0.1keV$.
- Charge exchanges between neutral hydrogen region and ionized region. New X-ray lines. Possible explanation for the signal in Perseus (Presence of neutral filaments in the core of this cluster).

Possible candidates

- He-Like Cl line at 3.52 keV. But no presence of the stronger Cl lines at 3.27 keV and 3.44 keV.
- Underestimation of the K XVIII line (must be 10-20 times the estimated value to match with the unknown line).
- Non-equilibrium plasma: possible boost of the Ar XVII DR line at 3.62 keV (but not enough)
- S XVI recombination edge at 3.494 keV. Significant for colder electron $T_e \sim 0.1keV$.
- Charge exchanges between neutral hydrogen region and ionized region. New X-ray lines. Possible explanation for the signal in Perseus (Presence of neutral filaments in the core of this cluster).

Are the K XVIII lines bananas?

Jetlema et al 2014: "Dark matter searches going bananas: the contribution of Potassium (and chlorine) to the 3.5 keV line"

- Claim of an underestimation of the K XVIII lines at 3.47 keV and 3.51 keV partially due to an inconsistent multi-temperature model (too high temperature) in Bulbul et al (highy controversial)
- Ca XX/CaXIX (for MOS spectrum) ratio leads to $T_e = 3.5keV$. Minimal $T_e = 5.9keV$ above in Bulbul et al. Effect on the emissivities? Bulbul et al answer: no significant change.
- Leads to a battle in arxiv.

Explanation by underestimated known plasma lines

Evidence for an unknown line at 3.5 keV

- Boyarski et al 2014: Another XMM analysis a 3.51 keV additional lines in the Perseus cluster (outskirt region), in M31 (Andromeda) and in the Galactic center but in this last case can't exclude an explanation by a plasma line.
- Chandra detection in Bulbul et al : significant additional line in Perseus.
- Riemer-Sorensen 2014: No evidence for an additional line in the center of our galaxy.

Evidence for an unknown line at 3.5 keV

- Boyarski et al 2014: Another XMM analysis a 3.51 keV additional lines in the Perseus cluster (outskirt region), in M31 (Andromeda) and in the Galactic center but in this last case can't exclude an explanation by a plasma line.
- Chandra detection in Bulbul et al : significant additional line in Perseus.
- Riemer-Sorensen 2014: No evidence for an additional line in the center of our galaxy.

Suzaku and the Perseus cluster

Tamura et al 2015:

- No evidence for an additional line in the Perseus cluster.
- Line explained by instrumental calibration errors/ continuum modeling issues

Urban et al 2015 :

- Find the additional line in the Perseus cluster. Consistent with Bulbul et al.
- Evolution of the flux between a small radius and a larger radius measurement inconsistent with a dark matter decay. Line due to bad modeling of the complex Perseus spectra?
- Measurement of $sin^2(2\theta)$ with the Perseus core signal must lead to a significant signal in Coma, Virgo and Ophiuchus. But nothing is found.

Explanation by underestimated known plasma lines

Evidence for an unknown line at 3.5 keV

- Boyarski et al 2014: Another XMM analysis a 3.51 keV additional lines in the Perseus cluster (outskirt region), in M31 (Andromeda) and in the Galactic center but in this last case can't exclude an explanation by a plasma line.
- Chandra detection in Bulbul et al : significant additional line in Perseus.
- Riemer-Sorensen 2014: No evidence for an additional line in the center of our galaxy.

Suzaku and the Perseus cluster

Tamura et al 2015:

- No evidence for an additional line in the Perseus cluster.
- Line explained by instrumental calibration errors/ continuum modeling issues

Urban et al 2015 :

- Find the additional line in the Perseus cluster. Consistent with Bulbul et al.
- Evolution of the flux between a small radius and a larger radius measurement inconsistent with a dark matter decay. Line due to bad modeling of the complex Perseus spectra?
- Measurement of $sin^2(2\theta)$ with the Perseus core signal must lead to a significant signal in Coma, Virgo and Ophiuchus. But nothing is found.

Work in progress

- Perseus cluster: Evidence for a plasma line.
- Rest of the sample: an open question.
- Astro-H launch in 2015/early 2016: better resolution and sensitivity.
- Radial distribution of the additional emission; proportional to the mass density (DM decay line) or proportional to the mass density squared (plasma line)? A way to discriminate.

Thanks for your attention!